Wireless Personal Communications (2019) 108:1079–1096
https://doi.org/10.1007/s11277-019-06455-2

Overlay Cognitive Radio Based on OFDM with Channel Estimation Issues

Ahmed Abdou[1] · **Ali Abdo**[2] · **Ali Jamoos**[1]

Published online: 9 May 2019
© Springer Science+Business Media, LLC, part of Springer Nature 2019

Abstract
Cognitive radio (CR) has been proposed as a technology to improve the spectrum efficiency by giving an opportunistic access of the licensed-user spectra to unlicensed users. We consider an overlay CR consisting of a primary macro-cell and cognitive small cells of cooperative secondary base stations (SBS). We suggest studying a CR where an orthogonal frequency division multiplexing is used for both the primary users (PU) and the secondary users (SU). In order to cancel the interferences, a precoding is required at the SBS. Therefore, we first derive the interferences expression due to SU at the PU receiver. Then, zero forcing beamforming (ZFBF) is considered to cancel the interferences. However, applying ZFBF depends on the channels between the SBS and the PU. A channel estimation is hence necessary. For this purpose, we propose to approximate the channel by an autoregressive process (AR) and to consider the channel estimation issue by using a training sequence. The received signals, also called the observations, are considered to be disturbed by an additive white measurement noise. In that case, the AR parameters and the channel can be jointly estimated from the received noisy signal by using a recursive approach. Nevertheless, the corresponding state space representation of the system is non-linear. Then, we propose to carry out a complementary study by compare non-linear Kalman filter based approaches.

Keywords Overlay cognitive radio · OFDM · Channel estimation · Nonlinear Kalman filters

✉ Ahmed Abdou
aabdou@staff.alquds.edu

Ali Abdo
aabdo@birzeit.edu

Ali Jamoos
ali.jamoos@staff.alquds.edu

[1] Department of Electronic and Communication Engineering, Najjad Zeenni Faculty of Engineering, Al-Quds university, P.O Box 20002, Jerusalem, Palestine

[2] Department of Electrical and Computer Engineering, Engineering Faculty, Birzeit University, Ramallah, Palestine

1 Introduction

With the increasing number of wireless devices, the radio spectrum becomes more and more overcrowded. At the same time, some studies show that wide ranges of the spectrum are rarely used most of the time, unlike other bands [1–3]. Those unused portions of the spectrum are licensed and thus can only be used by the license owners. In order to meet the needs and optimize the use of the resources, a novel technology is required and could benefit from the unused spectrum. In that context, cognitive radios (CRs) have been firstly proposed by Mitola [4] to allow spectrum reuse. Indeed, a CR is an intelligent radio that is dynamically configured to detect and then to use the available spectrum bands to transmit data. In that case, two systems must coexist:

1. The primary system (PS) which is a system already in operation using a license of the spectrum such as global system for mobile communications (GSM), long term evolution (LTE) system, etc. It cannot be modified.
2. The secondary system (SS) which aims at using the free resources of the PS in order to transmit its own data. CRs compose the SS.

They respectively involve the so-called primary users (PU) and secondary users (SU) who have to share the spectrum.

This can be done in various ways [5] and has led to three main families of CR systems: the so-called "interweave" , "underlay" and "overlay" modes. Thus, in the "interweave" mode, opportunistic communications consist in searching the spectrum holes left by the PU. It has been for instance used in [6–8]. In the "underlay" mode, PU and SU are allowed to simultaneously transmit data. It should be noted that the SU signal must be spread over a bandwidth large enough to ensure that the amount of interferences caused to the PU is under a certain threshold. This mode is useful for short range communications. For more details, the reader can for instance refer to [9–11]. In the "overlay" mode, some *a priori* information of the PU at the secondary transmitter is required to mitigate the interferences at the secondary receiver. It has led to several studies[1] such as in [13–16].

In this research, we consider the overlay CR mode. Therefore, the channel estimation issue is addressed. Indeed, the estimation of the fading process is essential to achieve symbol detection at the receiver. In this paper, we consider the training sequence/pilot-aided techniques family. Thus, during the training mode, the training symbols make it possible to estimate the channel. Then, during the decision mode, the channel estimates and prediction are used for symbol detection.

A brief state of the art about channel modeling can be found in [17–21] etc. In this paper, we focus our attention on the autoregressive (AR) model [22, 23] to represent the real and imaginary parts of the stationary channel.

When estimating the channel based on a training sequence and an *a priori* AR modeling, the received signal is used. It must be clearly expressed. Usually, it corresponds to the transmitted signal disturbed by the influences of the channel and an additive noise. The standard assumption is to consider the additive noise as a white[2] sequence [22, 23]. In that

[1] In [12], the authors suggest switching from an overlay CR mode to an underlay one.

[2] The case of an additive measurement colored noise, and more particularly a noise that can be modeled by a moving average (MA) process is also considered in [26].

case, the AR parameters and the channel can be jointly estimated from the received noisy signal during the training mode by using a recursive approach. As the corresponding state space representation of the system is non-linear, methods such as the extended Kalman filter (EKF), the second order EKF (SOEKF) [24] and unscented Kalman filter (UKF) [25] can be used. Several other variants of Kalman filtering have been proposed in the literature, but they have not been compared one another. Therefore, we propose to carry out a complementary study by investigating the relevance of the quadrature Kalman filter (QKF) [27] and the cubature Kalman filter (CKF) [28].

The rest of the paper is organized as follows. Section 2 overviews the system model of the system. The channel estimation is studied in Sect. 3. Simulation results are illustrated in Sect. 4. Finally, conclusion remarks are drawn in Sect. 5 and the appendices are addressed in Sect. 1.

2 System Model

Small cell is a new trend in cellular communications. In any cell, smaller base stations can be inserted to aid capacity and coverage. Such smaller base stations are called small cells. A small cell can be inserted on lamp posts, trees and buildings. These low consumption radio transceivers are cheap and need low power. Therefore, if one of these base stations is ceased, the others around it compensate its loss. To do this, these small cells must be intelligent and have a real-time situations awareness.

Unlike micro-cells, small cells aim at intelligently reusing the same band as the micro-cells and hence maximizing the spectral efficiency. A question could be asked: what is the useful of the small cells that allow to operate side by side with micro-cells and cellulars and sharing the same band and the same radio access technology?

Indeed, if the whole radio network is seen from the CR perspective, i.e., macro-base stations and its users, acting as the primary system, are protected from interferences. In addition, the cooperative small-cells and its users, acting as the secondary system, can accept interferences from the macro-base stations. Then, the idea of dynamic spectrum access comes as a candidate solution.

In the next section, the small cells are applied in CR scenario.

2.1 CR Based OFDM in a Small Cell

Let us consider a primary macro-cell composed of virtual MIMO networks, based on small-cells SBS cooperation as shown in Fig. 1. In this system, we consider a SISO PS whereas the SS consists of U SBS's each equipped with A antennas. The PS and the SS are CP-OFDM system with N subcarriers for each. The effect of the different CFO's of each SBS on the received signal at the PU are now considered.

The received signal at the PU receiver $r_p(n)$, where the CFO between the PBS and the PU is assumed to be estimated and removed at the receiver[3], can be expressed as follows:

$$r_p(n) = x_p(n) * h_p(n) + i(n) + b(n) \tag{1}$$

where the interferences $i(n)$ is defined as:

[3] For more information, the reader may refer to [29, 30].

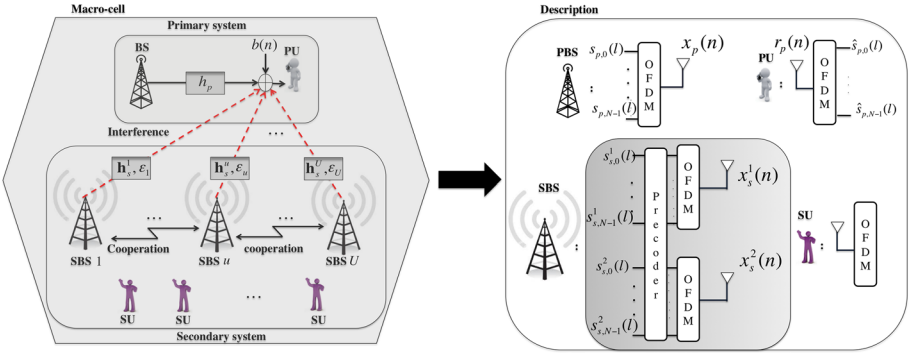

Fig. 1 General case for overlay CR system based on CP-OFDM for PS and small-cell SBS cooperation

$$i(n) = \sum_{a=1}^{A} \sum_{u=1}^{U} x_s^{a,u}(n) * h_s^{a,u}(n) e^{j2\pi\epsilon_u \frac{n}{N}} \tag{2}$$

and $x_s^{a,u}(n)$ is the secondary transmitted CP-OFDM signal of the a^{th} antenna of the u^{th} SBS and $h_s^{a,u}(n)$ is the channel between the PU and the a^{th} antenna of u^{th} SBS. In addition, ϵ_u is the difference between the normalized CFO of the PBS and the normalized CFO of the u^{th} SBS. It should be noted that (2) can no longer be presented as a simple multiplication because of the effect of CFO that breaks the subcarrier orthogonality. Indeed, the k^{th} subcarrier at the receiver is affected by the neighbours subcarriers. Therefore, the interferences after the FFT of the PU receiver can be written as follows:

$$\widehat{X}_{p,k} = s_{p,k} H_{p,k} + FFT_k\{b(n)\}_0^{N-1} + \sum_{u=1}^{U} I_k^u \tag{3}$$

where

$$I_k^u = FFT_k\{e^{j2\pi\epsilon_u \frac{n}{N}} \sum_{a=1}^{A} x_s^{a,u}(n) * h_s^{a,u}(n)\}_0^{N-1} \tag{4}$$

At this stage, let us recall the mathematical representation of the transmitted CP-OFDM transmitted signal, the transmitted block can be written as follows:

$$x_p(n) = \frac{1}{\sqrt{N}} \sum_{m=0}^{N-1} s_m(l) e^{j2\pi \frac{mn}{N}} = IFFT\{s_m(0)\}_0^{N-1} \tag{5}$$

where $IFFT\{\ \}_0^{N-1}$ is the normalized $IFFT$ of the transmitted symbols $s_m(l)$ of the m^{th} carrier and l^{th} symbol. Using (5), and by taking the 0^{th} CP-OFDM symbol, (4) can be expressed as:

$$I_k^u = FFT\{e^{j2\pi\epsilon_u \frac{n}{N}} \frac{1}{\sqrt{N}} \sum_{a=1}^{A} \sum_{m=0}^{N-1} s_{m,s}^{a,u} e^{j2\pi m \frac{n}{N}} * h_s^{a,u}(n)\}_k \tag{6}$$

$$=\frac{1}{\sqrt{N}}\sum_{n=0}^{N-1}\sum_{a=1}^{A}\Big(\sum_{m=0}^{N-1}s_{m,s}^{a,u}e^{j2\pi m\frac{n}{N}} * h_s^{a,u}(n)\Big)e^{-j2\pi n\frac{(k-\epsilon_u)}{N}} \tag{7}$$

The above equation can be reformulated as follows:

$$=\frac{1}{\sqrt{N}}\sum_{a=1}^{A}\sum_{n=0}^{N-1}\sum_{m=0}^{N-1}\Big(\sum_{n'=-\infty}^{+\infty}s_{m,s}^{a,u}h_s^{a,u}(n')e^{-j2\pi m\frac{n'}{N}}\Big)e^{-j2\pi n\frac{(k-\epsilon_u-m)}{N}} \tag{8}$$

In order to apply the Fourier transform, it is possible to add a rectangular window $w(n)$ on (8) as follows:

$$=\frac{1}{\sqrt{N}}\sum_{a=1}^{A}\sum_{n=-\infty}^{+\infty}\Big(\sum_{m=0}^{N-1}s_{m,s}^{a,u} * h_s^{a,u}(n)e^{-j2\pi\frac{nm}{N}}\Big)e^{-j2\pi n(\frac{k-\epsilon_u-m}{N})}.w(n) \tag{9}$$

where

$$w(n)=\begin{cases}1, & n=0,1,...,N-1\\ 0, & otherwise\end{cases} \tag{10}$$

Hence it can be expressed as follows:

$$I_k^u=\sum_{a=1}^{A}\sum_{m=0}^{N-1}s_{m,s}^{a,u}H_s^{a,u}(f+\frac{m}{N}) * W(f)|_{f=\frac{(k-\epsilon_u-m)}{N}} \tag{11}$$

where $H_s^{a,u}(f)$ denote the FFT of $h_s^{a,u}(n)$ and $W(f)=\sqrt{N_p}\text{sinc}(fN_p)e^{-j2\pi f\frac{N_p}{2}}$. By assuming we can neglect the influence of the convolution $W(f)|_{f=\frac{(k-\epsilon_u-m)}{N}}$, (11) can be rewritten as follows:

$$I_k^u=\sum_{a=1}^{A}\sum_{m=0}^{N-1}s_{m,s}^{a,u}H_s^{a,u}(f+\frac{m}{N})|_{f=\frac{(k-\epsilon_u-m)}{N}} \tag{12}$$

One can notice that the $N-1$ subcarriers in the SU system are considered even if some SU subcarriers do not interfere much with the k^{th} PU subcarrier. In the next sections, the ZFBF design is presented. Then, we propose to make an approximation in order to select the most interfering SU subcarriers around the k^{th} PU subcarrier.

For that reason and for the sake of simplicity, let us denote for $m=0,\cdots,N-1$:

$$f_{k,m}=\frac{(k-\epsilon_u-m)}{N}=f_{k,0}-\frac{m}{N} \tag{13}$$

2.2 Designing the ZFBF

To perform the ZFBF, let us set all the symbols to be equal[4] i.e., $s^u_{m,s} = s^{a,u}_{m,s}$. In that case (12) can be rewritten in a matrix form as follows:

$$(\mathbf{H}^u_k.\mathbf{Z}^u_k)^T\mathbf{S}^u = 0 \tag{14}$$

where

$$\mathbf{S}^u = \left[s^u_{m-N_{sc},s} \cdots s^u_{m+N_{sc},s}\right]^T \tag{15}$$

with N_{sc} the considered neighbouring subcarrier that affect on the k^{th} PU subcarrier. In addition, $\mathbf{H}^u_k$ is the $(2N_{sc}+1)\times A$ matrix that contains all the channels interfering with the k^{th} PU subcarrier:

$$\mathbf{H}^u_k = \begin{bmatrix} H^{1,u}_s(f_{k,0}) & \cdots & H^{A,u}_s(f_{k,0}) \\ \vdots & \ddots & \vdots \\ H^{1,u}_s(f_{k,0}) & \cdots & H^{A,u}_s(f_{k,0}) \end{bmatrix} \tag{16}$$

and the column vector $\mathbf{Z}^u_k = \begin{bmatrix} Z^{1,u}_k & Z^{2,u}_k & \ldots & Z^{A,u}_k \end{bmatrix}^T$ with length $(A\times 1)$ storing the beamformers.

To solve this issue, we suggest finding a set $\{Z^{a,u}_k\}$ that satisfies:

$$\mathbf{H}^u_k\mathbf{Z}^u_k = \mathbf{0} \tag{17}$$

In addition to the trivial solution $\mathbf{Z}^u_k = \mathbf{0}$, another solution is based on a property of the singular value decomposition (SVD) of the channel matrix $\mathbf{H}^u_k$ when $A > (2N_{sc}+1)$. Indeed, one thing the SVD of the matrix H^u_k does is to supply an orthonormal basis of its kernel[5]. Therefore, provided that the channel matrix is *a priori* known or estimated, the SVD of the channel matrix $\mathbf{H}^u_k$ can be computed. Indeed, the SVD of the matrix $\mathbf{H}^u_k$ satisfies:

$$\mathbf{H}^u_k = \mathbf{U}\boldsymbol{\Sigma}\mathbf{V}^T \tag{18}$$

where $\mathbf{U}$ is a $(N_{sc}+1)\times(N_{sc}+1)$ orthogonal matrix whose columns are the left singular vectors $\{\mathbf{U}_i\}_{i=1,\cdots,N_{sc}+1}$, $\boldsymbol{\Sigma}$ is the $(N_{sc}+1)\times A$ pseudo-diagonal matrix with diagonal entries σ_i corresponding to the singular values of $\mathbf{H}^u_k$ and $\mathbf{V}^T$ is a $A\times A$ orthogonal matrix whose columns are the right singular vector $\{\mathbf{V}_i\}_{i=1,\cdots,A}$.

When $A > N_{sc}+1$,

$$\mathbf{H}^u_k\mathbf{V}_i = \sigma_i\mathbf{U}_i \qquad \text{for } i = 1,\cdots,N_{sc}+1 \tag{19}$$

otherwise,

$$\mathbf{H}^u_k\mathbf{V}_i = 0 \tag{20}$$

Therefore, one can define the kernel of $\mathbf{H}^u_k$. More particularly, using the SVD (18) and pre-multiplying the matrix $\mathbf{H}^u_k$ by the p^{th} right singular vector $\mathbf{V}_p$, where $p > N_{sc}+1$, one has:

$$\mathbf{H}^u_k\mathbf{V}^T_p = \mathbf{U}\begin{bmatrix} \sigma_1 & \cdots & 0 & 0 & \cdots & 0 \\ \vdots & \ddots & 0 & \vdots & & \vdots \\ 0 & \cdots & \sigma_{N_{sc}+1} & 0 & & 0 \end{bmatrix}[\mathbf{V}_1 \cdots \mathbf{V}_A]^T\mathbf{V}^T_p = 0 \tag{21}$$

[4] This assumption is considered to perform the ZFBF. This assumption does not decrease the spectral efficiency as it is in the ZFBF context and it is done by many authors such as [15, 31].

[5] As an alternative to SVD, QR factorization could be also considered.

It can be shown that when Z_k^u is the p^{th} right singular vector, (17) is satisfied. Then, $\mathbf{Z}_k^u$ can be set to the value of the p^{th} right singular vector, where $2N_{sc}+1 < p \leq A$. In the next section, a complementary study for non-linear Kalman filter based approaches is considered as a main issue to apply ZFBF.

3 Channel Estimation Issue

In this section, the channel[6] is assumed to be approximated by a p^{th} order AR process as follows:

$$h(n) = -\sum_{i=1}^{p} a_i h(n-i) + u(n) \tag{22}$$

where $\{a_i\}_{i=1,\cdots,p}$ are the AR parameters and the driving process $u(n)$ is a zero-mean white Gaussian process with variance $\sigma_u^2(p)$.

Let us consider an OFDM system. The received signal[7] on each subcarrier can be expressed as a simple multiplication between the channel and the symbol as follows:

$$y(n) = h(n)s(n) + b(n) \tag{23}$$

where $s(n)$ is the transmitted symbol. In addition, the noise $b(n)$ in (23) is a zero-mean white noise with a variance σ_b^2 uncorrelated with $u(n)$.

In the following, two cases are considered:

1. The AR parameters have been *a priori* estimated, whereas the channel is unknown;
2. Both the AR parameters and the channel are unknown.

3.1 Estimation of the Fading Channel When the AR Parameters Have Been *a priori* Estimated

Let us first assume that the AR parameters $\{a_i\}_{i=1,\cdots,p}$ have been *a priori* estimated by using some approaches such as high-order Yule-Walker equation (HOYW) when the observations disturbed by an additive white noise. The reader can read [22] and [26]. In that case, Kalman filter can be used to estimate the fading process by minimizing the estimation error variance. Therefore, the state vector $\mathbf{h}(n)$ can be written as follows:

$$\mathbf{h}(n) = \begin{bmatrix} h(n) & h(n-1) \cdots h(n-p+1) \end{bmatrix}^T \tag{24}$$

Given the state vector (24), the state space representation of (22) and (23) can be expressed that way:

[6] For the sake of simplicity $h_s^{a,u}(n)$ in (2) is written as $h(n)$.

[7] As mentioned before that for sake of simplicity and without loss of generality, we deal with the real part only, i.e., the real part of $r(n)$, $h(n)$, $s(n)$ and $b(n)$ are considered. The same procedure can be done when the imaginary parts are considered.

$$\mathbf{h}(n) = \mathbf{F}(n)\mathbf{h}(n-1) + \mathbf{G}u(n) \tag{25}$$

and

$$y(n) = \mathbf{S}^T(n)\mathbf{h}(n) + b(n) \tag{26}$$

where $\mathbf{F}(n)$ is the transition companion matrix defined as follows:

$$\mathbf{F}(n) = \begin{bmatrix} -a_1 & \cdots & -a_{p-1} & -a_p \\ 1 & 0\cdots & 0 & 0 \\ \vdots & \ddots & & \vdots \\ 0 & \cdots & 1 & 0 \end{bmatrix} \tag{27}$$

and $\mathbf{G} = [1 \quad \underbrace{0 \cdots 0}_{p-1}]^T$. In addition, the observation vector is $\mathbf{S}^T(n) = [s(n) \quad \underbrace{0 \cdots 0}_{p-1}]$ and $b(n)$ and $u(n)$ assumed to be uncorrelated with the elements of the initial state vector $\mathbf{h}(0)$. The above equations define the state space representation of one-carrier fading channel system. At that stage, a standard Kalman (see "Appendix 1") filtering algorithm can be carried out to provide the estimation $\hat{\mathbf{h}}(n|n)$ of the state vector $\mathbf{h}(n)$ given the set of observations $\{y(n)\}_{n=1,\cdots N}$.

The next section presents the case when both the AR parameters and the channel are unknown.

3.2 Joint Estimations of the AR Parameters and the Channel (Nonlinear Estimation Approaches)

In this section, the AR parameters and the channel are jointly estimated. In that case, the state vector contains the unknown values and can be written as follows:

$$\boldsymbol{\varphi}(n) = \left[\boldsymbol{\theta}_h(n)^T \quad \mathbf{h}(n)^T\right]^T \tag{28}$$

where $\boldsymbol{\theta}_h(n) = \left[a_1 \cdots a_p\right]^T$ and $\mathbf{h}(n)$ is defined in (24). In addition, the AR-process parameters do not vary in time. Therefore, the vector storing these quantities are updated as follows:

$$\boldsymbol{\theta}_h(n) = \boldsymbol{\theta}_h(n-1) \tag{29}$$

Given (25), (28) and (29), $\boldsymbol{\varphi}(n)$ can be updated as follows:

$$\boldsymbol{\varphi}(n) = \boldsymbol{\Phi}\left(\boldsymbol{\varphi}(n-1); n, n-1\right) + \boldsymbol{\Gamma}u(n) \tag{30}$$

where $\boldsymbol{\Phi}$ is a non-linear function and $\boldsymbol{\Gamma}(n) = [\underbrace{0 \cdots 0}_{p} \quad 1 \quad \underbrace{0 \cdots 0}_{p-1}]^T$.

In the above equation, the non-linear function $\boldsymbol{\Phi}$ can be expressed as follows:

$$\boldsymbol{\Phi}\left(\boldsymbol{\varphi}(n-1); n, n-1\right) = \mathbf{D}\boldsymbol{\varphi}(n-1) + \mathbf{E}^T\boldsymbol{\varphi}^T(n-1)\mathbf{G}\boldsymbol{\varphi}(n-1) \tag{31}$$

with:

$$\mathbf{D} = \begin{bmatrix} \mathbf{I}_p & \mathbf{0}_{p\times(p-1)} & \mathbf{0}_{p\times 1} \\ \mathbf{0}_{1\times p} & \mathbf{0}_{1\times(p-1)} & 0 \\ \mathbf{0}_{(p-1)\times p} & \mathbf{I}_{(p-1)} & \mathbf{0}_{(p-1)\times 1} \end{bmatrix} \tag{32}$$

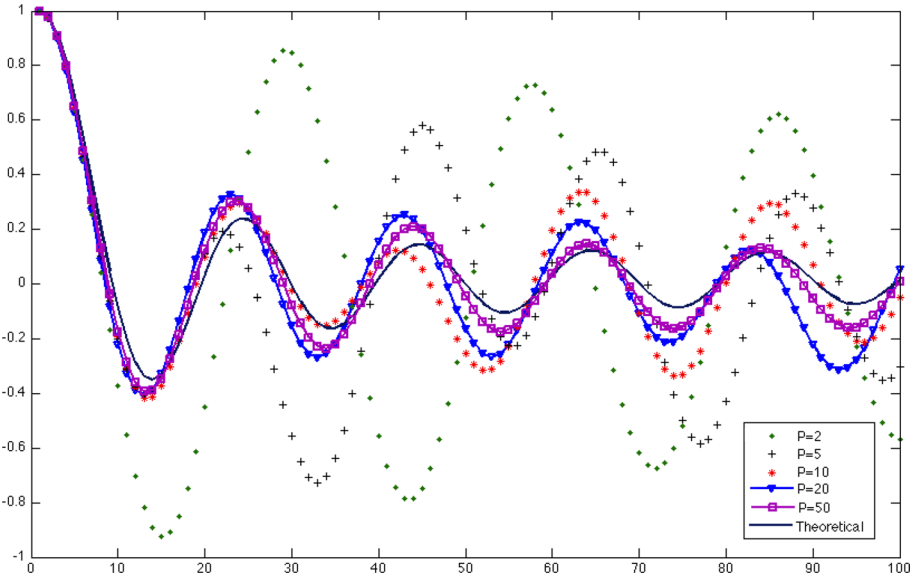

Fig. 2 Autocorrelation of the channel for different AR-process order p

$$\mathbf{E} = \begin{bmatrix} \mathbf{0}_{1\times p} & 1 & \mathbf{0}_{1\times(p-1)} \end{bmatrix} \tag{33}$$

and

$$\mathbf{G} = \begin{bmatrix} \mathbf{0}_{p\times p} & -\mathbf{I}_p \\ \mathbf{0}_{p\times p} & \mathbf{0}_{p\times p} \end{bmatrix} \tag{34}$$

The observation equation can be written as follows:

$$y(n) = \mathbf{E'}^T(n)\mathbf{h}(n) + b(n) \tag{35}$$

where $\mathbf{E'}^T(n) = \begin{bmatrix} \mathbf{0}_{1\times p} & s(n) & \mathbf{0}_{1\times(p-1)} \end{bmatrix}$.

As the state space representation described in (30) and (35) is non-linear, one can use the EKF, the SOEKF and the UKF. For more information about these algorithms, see the "Appendices 2–4". In addition, we suggest in this research to investigate the relevance of other variants such as the QKF and the CKF, see "Appendices 5–7".

4 Simulation Results

In this section, we carry out a comparative study on the estimation of OFDM fading channels between several methods based on Kalman filter. We consider an OFDM system with QPSK modulation and 64 subcarriers. Moreover, the channel is Rayleigh fading channel with a maximum Doppler frequency chosen randomly between 50 and 150 Hz.

Concerning the channels in our simulations, they are generated by using p^{th}-order AR process. In order to see the influence of the order on the channel properties, Fig. 2 provides the estimation of the correlation function of the channel for various AR-process orders,

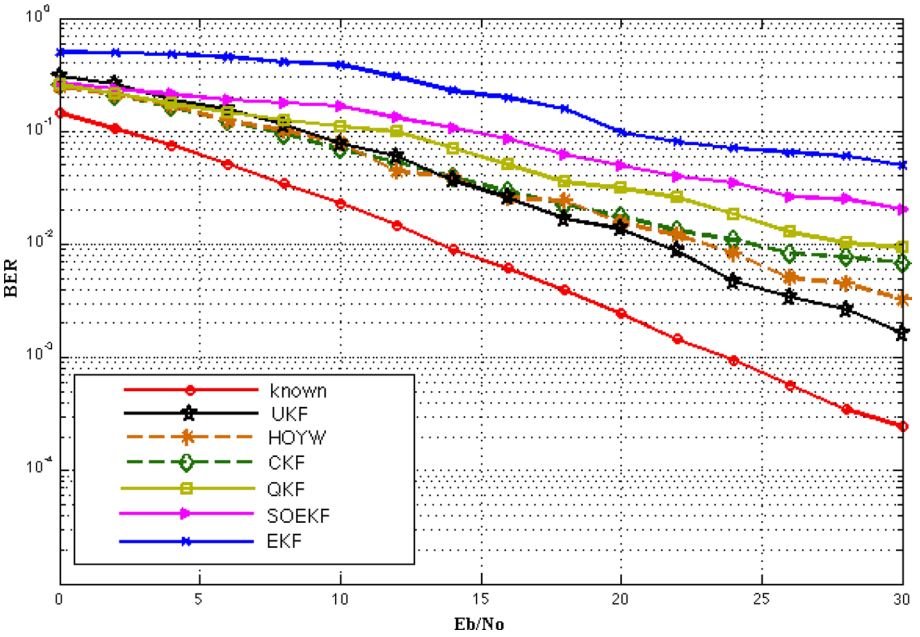

Fig. 3 BER performance versus SNR of the OFDM system with $p = 2$

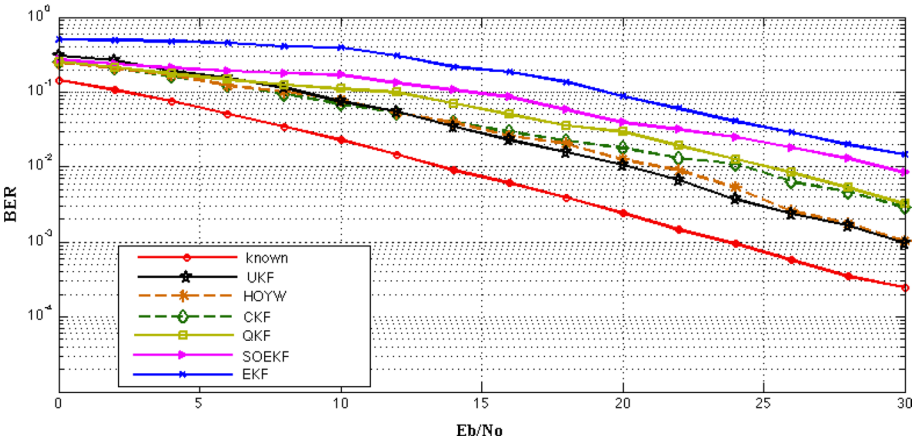

Fig. 4 BER performance versus SNR of the OFDM system with $p = 5$

namely p =2, 5, 10, 20 and 50. In addition, these estimations are compared with the theoretical autocorrelation of the channel. We can notice that the higher the order is, the more accurate the resulting correlation function is. As pointed out by Baddour, an order of 50 can be a compromise to simulate the channels in the transmission chain.

Concerning the receiver, by considering a training sequence mode, we propose to analyze the BER performance vs SNR of the following methods:

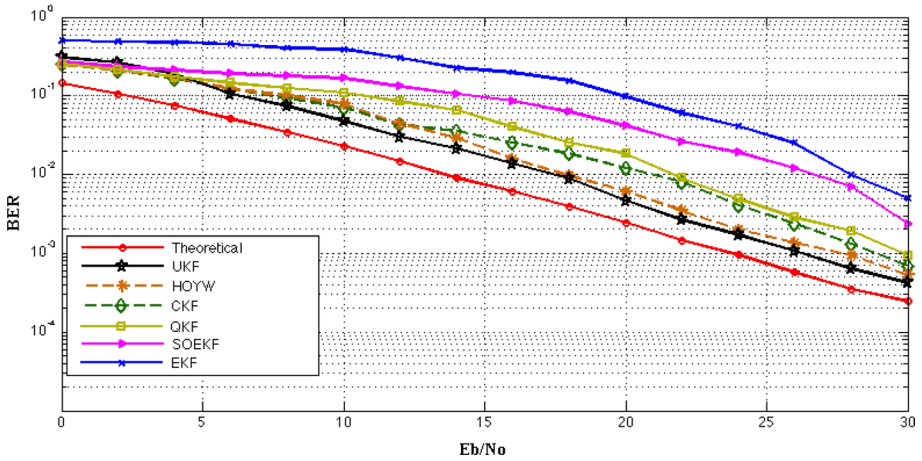

Fig. 5 BER performance versus SNR of the OFDM system with $p = 10$

1. Kalman filter with known AR parameters (known),
2. The UKF,
3. HOYW-based approach,
4. The QKF "with a quadrature point equal to 3" and the CKF.
5. The EKF and the SOEKF,

In addition, we study several assumptions on the AR channel order. Thus, p is set to 2, 5 and 10 respectively in Figs. 3, 4 and 5.

On the one hand, it is true that when the highest AR-process order p is considered, the lower BER is obtained. However, choosing a higher order leads to a higher number of AR parameters to be estimated and hence a higher computational cost. Choosing the order of the AR process p equal to 4 or 5 can be a trade-off between computational cost and performance in terms of BER.

On the other hand, as shown in the Figs. 3 , 4 and 5, the QKF[8] and the CKF do not lead to major improvements for channel estimation. Both have higher computational costs than the other approaches. It should be noted that the UKF and the HOYW give the lowest BER compared with the other approaches.

5 Conclusions and Perspectives

In this paper, we have investigated the relevance of the performing the precoding, i.e., zero-forcing beamforming (ZFBF) by taking into account the signal at the receiver after OFDM demodulation has the advantages of decreasing the effect of the carrier frequency offset (CFO) and hence reducing the number of subcarriers needed for the interference cancellation. However, ZFBF depends on the channels between the SS and the PS. They must

[8] The higher the chosen number of quadrature points is, the more accurate the results are.

hence be known or estimated. Therefore, we focus our attention on the channel estimation where the channel is approximated by an autoregressive (AR) process. We focus our attention on channels disturbed by an additive white noise were considered. This issue has been addressed by several authors in the literature. Our contribution was to analyze the performance of variants of Kalman filters, more particularly, the quadrature Kalman filter (QKF) and the cubature Kalman filter (CKF). A comparative study was carried out between: the extended Kalman filter (EKF), the second-order EKF (SOEKF), the unscented Kalman filter (UKF), the QKF and the CKF. The above approaches were also compared with the overdetermined high-order Yule-Walker (HOYW) equations and the Kalman filter when the AR parameters are known. The comparative study showed that the QKF and the CKF do not lead to major improvements for channel estimation whereas both have higher computational costs than the other methods. In addition, the UKF and the HOYW equations give the lowest BER compared with the other approaches. Since non-linear estimation methods are crucial in signal processing, a great deal of attention is paid to design a new approach. Therefore, we could in the future study another novel nonlinear filter named sparse-grid quadrature filter (SGQF) and compare it with the above nonlinear estimators.

Appendices

Kalman filter (KF) has been used in a wide range of applications, from speech enhancement to time-varying autoregressive parameters tracking, from biomedical applications to mobile communications. More particularly, in this paper, Kalman filter can be used to estimate the channel (see "Appendix 1"). In the "Appendices 2 and 3", we recall how to address the estimation of the state vector by using the extended Kalman filter (EKF) or the second-order EKF (SOEKF), where Taylor series expansion is used. It should be noted that the state noise and the measurement noise are still assumed to be Gaussian. In "Appendix 4", the UKF was proposed as an alternative to the EKF to avoid the linearization step. Like the UKF, the Quadrature Kalman filter (QKF) and Cubature Kalman filter (CKF) are a sigma point Kalman filter (SPKF) (See "Appendix 5"). The main difference between QKF, CKF and UKF is the way to choose the sigma points. In "Appendices 6 and 7" deal with how to choose the sigma points. Indeed, in QKF the sigma points are chosen by using the Gauss-Hermite quadrature where CKF differs from QKF by the considered way of approximation.

Appendix 1: Kalman filter

- initialize the value of $\hat{\mathbf{x}}(0|0)$ and $\mathbf{P}(0|0)$.

The prediction step

- update the state vector:

$$\hat{\mathbf{x}}(n|n-1) = \mathbf{F}(n)\hat{\mathbf{x}}(n-1|n-1)$$

- update the error covariance matrix:

$$\mathbf{P}(n|n-1) = \mathbf{F}(n)\mathbf{P}(n-1|n-1)\mathbf{F}^H(n) + \mathbf{G}\mathbf{Q}\mathbf{G}^H$$

The filtering step

- update the Kalman gain:

$$\mathbf{K}(n) = \mathbf{P}(n|n-1)\mathbf{H}(n)^H\left(\mathbf{H}(n)\mathbf{P}(n|n-1)\mathbf{H}(n)^H + \mathbf{R}\right)^{-1}$$

- update the state vector:

$$\hat{\mathbf{x}}(n|n) = \hat{\mathbf{x}}(n|n-1) + \mathbf{K}(n)(\mathbf{y}(n) - \mathbf{H}(n)\hat{\mathbf{x}}(n|n-1))$$

Appendix 1: Kalman filter

- finally, update the error covariance matrix:

$\mathbf{P}(n|n) = \{\mathbf{I}_U - \mathbf{K}(n)\mathbf{H}(n)\}\mathbf{P}(n|n-1)$

Appendix 2: Extended Kalman filter

- initialize the value of $\hat{\mathbf{x}}(0|0)$ and $\mathbf{P}(0|0)$.

- calculate the Jacobian matrix $\nabla_{\mathbf{x}}\mathbf{f}_n|_{\hat{\mathbf{x}}(n-1|n-1)}$.

- update the *a priori* state vector:

$\hat{\mathbf{x}}(n|n-1) = \mathbf{f}_n(\hat{\mathbf{x}}(n-1|n-1))$

- update the *a priori* error covariance matrix:

$\mathbf{P}(n|n-1) = \nabla_{\mathbf{x}}\mathbf{f}_n|_{\hat{\mathbf{x}}(n-1|n-1)}\mathbf{P}(n-1|n-1)\nabla_{\mathbf{x}}\mathbf{f}_n^H|_{\hat{\mathbf{x}}(n-1|n-1)} + \mathbf{GQG}^H$

- calculate the Jacobian matrix $\nabla_{\mathbf{x}}\mathbf{h}_n|_{\hat{\mathbf{x}}(n|n-1)}$.

- update the Kalman gain $\mathbf{K}(n)$:

$\mathbf{K}(n) = \mathbf{P}(n|n-1)\nabla_{\mathbf{x}}\mathbf{h}_n^H|_{\hat{\mathbf{x}}(n|n-1)}\left(\nabla_{\mathbf{x}}\mathbf{h}_n|_{\hat{\mathbf{x}}(n|n-1)}\mathbf{P}(n|n-1)\nabla_{\mathbf{x}}\mathbf{h}_n^H|_{\hat{\mathbf{x}}(n|n-1)} + \mathbf{R}\right)^{-1}$

- deduce the *a posteriori* state vector:

$\hat{\mathbf{x}}(n|n) = \hat{\mathbf{x}}(n|n-1) + \mathbf{K}(n)\{\mathbf{y}(n) - \mathbf{h}_n(\hat{\mathbf{x}}(n|n-1))\}$

- finally, update the error covariance error matrix:

$\mathbf{P}(n|n) = \{\mathbf{I}_U - \mathbf{K}(n)\nabla_{\mathbf{x}}\mathbf{h}_n|_{\hat{\mathbf{x}}(n|n-1)}(n)\}\mathbf{P}(n|n-1)$

Appendix 3: Second-order extended Kalman filter

- calculate the Jacobian matrix $\nabla_{\mathbf{x}}\mathbf{f}_n|_{\hat{\mathbf{x}}(n-1|n-1)}$ and $\bar{\mathbf{f}}_{n-1}^{mean}$ using:

$\bar{\mathrm{f}}_n^{mean} = \mathbb{E}\{\bar{\mathbf{f}}_n|\mathbf{y}(0), \ldots, \mathbf{y}(n-1)\} = \sum_{u=1}^{U} \boldsymbol{\Theta}_u^{\mathrm{f}}\bar{\mathrm{f}}_{n,u}^{mean}$

with $\boldsymbol{\Theta}_u^{\mathrm{f}}$ is a $U \times 1$ vector with zeros everywhere except for the uth element which is equal to 1. see [24]

- update the *a priori* state vector:

$\hat{\mathbf{x}}(n|n-1) = \mathbf{f}_n(\hat{\mathbf{x}}(n-1|n-1)) + \frac{1}{2}\bar{\mathbf{f}}_{n-1}^{mean}$

- update the *a priori* error covariance matrix:

$\mathbf{P}(n|n-1) = \nabla_{\mathbf{x}}\mathbf{f}_n|_{\hat{\mathbf{x}}(n-1|n-1)}\mathbf{P}(n-1|n-1)\nabla_{\mathbf{x}}\mathbf{f}_n^H|_{\hat{\mathbf{x}}(n-1|n-1)} + \mathbf{GQG}^H$

- calculate the Jacobian matrix $\nabla_{\mathbf{x}}\mathbf{h}_n|_{\hat{\mathbf{x}}(n|n-1)}$ and $\bar{\bar{\mathbf{h}}}_n$ using (??).

- update the Kalman gain $\mathbf{K}(n)$ as follows:

$\mathbf{K}(n) = \mathbf{P}(n|n-1)\nabla_{\mathbf{x}}\mathbf{h}_n^H|_{\hat{\mathbf{x}}(n|n-1)}\left(\nabla_{\mathbf{x}}\mathbf{h}_n|_{\hat{\mathbf{x}}(n|n-1)}\mathbf{P}(n|n-1)\nabla_{\mathbf{x}}\mathbf{h}_n^H|_{\hat{\mathbf{x}}(n|n-1)} + \mathbf{R}\right)^{-1}$

- deduce the *a posteriori* state vector:

$\hat{\mathbf{x}}(n|n) = \hat{\mathbf{x}}(n|n-1) + \mathbf{K}(n)\{\mathbf{y}(n) - \mathbf{h}_n(\hat{\mathbf{x}}(n|n-1)) - \frac{1}{2}\bar{\bar{\mathbf{h}}}_n\}$

- finally, update the error covariance error matrix:

$\mathbf{P}(n|n) = \{\mathbf{I}_U - \mathbf{K}(n)\nabla_{\mathbf{x}}\mathbf{h}_n|_{\hat{\mathbf{x}}(n|n-1)}(n)\}\mathbf{P}(n|n-1)$

Appendix 4: Unscented Kalman filter

- calculate the sigma points:

$\mathcal{X}(n-1|n-1) = \left[\hat{\mathbf{x}}(n-1|n-1), \hat{\mathbf{x}}(n-1|n-1) \pm \left(\sqrt{(N_d+\lambda)\mathbf{P}(n-1|n-1)}\right)\right]$

- calculate the prediction of the system:

$\mathcal{X}(n-1|n-1) = \mathbf{f}_n(\mathcal{X}(n-1|n-1))$

- update the *a priori* mean is:

$\hat{\mathbf{x}}^-(n|n-1) = \sum_{\mathbf{m}=0}^{2U} w_{\mathbf{m}}^{(c0)}\mathcal{X}_{\mathbf{m}}(n|n-1)$

Appendix 4: Unscented Kalman filter

- update the *a priori* error covariance matrix:

$$\mathbf{P}(n|n-1) = \sum_{\mathbf{m}=0}^{2U} w_{\mathbf{m}}^{(c1)} \left[\mathcal{X}_{\mathbf{m}}(n|n-1) - \hat{\mathbf{x}}^{-}(n|n-1)\right]^{\star} + \mathbf{GQG}^{H}$$

- calculate $\hat{\mathbf{y}}^{-}(n|n-1)$:

$$\hat{\mathbf{y}}^{-}(n|n-1) = \sum_{m=0}^{2U} w_m^{c0} \mathcal{Y}_m(n|n-1)$$

where

$$\mathcal{X}(n|n-1) = \mathbf{f}_n(\mathcal{X}(n|n-1))$$

- update the Kalman gain:

$$\mathbf{K}(n) = \{\mathbf{P}^{\mathbf{xy}}\}\{\mathbf{P}^{\mathbf{yy}}\}^{-1}$$

where $\mathbf{P}^{\mathbf{yy}}$and $\mathbf{P}^{\mathbf{xy}}$ are defined as:

$$\mathbf{P}^{\mathbf{yy}}(n) = \sum_{m=0}^{2U} w_m^{c1} \left[\mathcal{Y}_m(n|n-1) - \hat{\mathbf{y}}^{-}(n|n-1)\right]^{\star} + \mathbf{R} \text{ and}$$

$$\mathbf{P}^{\mathbf{xy}}(n) = \sum_{m=0}^{2U} w_{\mathbf{m}}^{c1} \left[\mathcal{X}_m(n|n-1) - \hat{\mathbf{x}}^{-}(n)\right] \times \left[\mathcal{X}_m(n|n-1) - \hat{\mathbf{y}}^{-}(n|n-1)\right]$$

- update the state vector:

$$\hat{\mathbf{x}}(n|n) = \hat{\mathbf{x}}(n|n-1) + \mathbf{K}(n)\{\mathbf{y}(n) - \hat{\mathbf{y}}^{-}(n|n-1)\}$$

- update the error covariance matrix:

$$\mathbf{P}(n|n) = \mathbf{P}(n|n-1) - \mathbf{K}(n)\mathbf{P}^{\mathbf{yy}}(n)\mathbf{K}^{H}(n)$$

Appendix 5: Quadrature Kalman filter and Cubature Kalman Filter

Prediction:

- compute the Cholesky factor of $\mathbf{P}(n-1|n-1)$:

$$\mathbf{P}(n-1|n-1) = \mathbf{S}(n-1|n-1)\mathbf{S}(n-1|n-1)^{H}$$

- compute the sigma points and the weights according to "Appendix 6 (Gauss-Hermite quadrature points for QKF) or according to "Appendix 7" (the cubature points for CKF).

- evaluate the sigma points:

$$\mathcal{X}_l(n-1|n-1) = \hat{\mathbf{x}}(n-1|n-1) + \mathbf{S}(n-1|n-1)\xi_l$$

- propagate the sigma points through the non-linear update function:

$$\mathcal{X}_l^{*}(n|n-1) = \mathbf{f}_n(\mathcal{X}_l(n-1|n-1))$$

- estimate the *a priori* state vector by combining the *a posteriori* sigma points:

$$\hat{\mathbf{x}}(n|n-1) = \sum_l w_l \mathcal{X}_l^{*}(n-1|n-1)$$

- estimate the *a priori* estimation error covariance matrix:

$$\mathbf{P}(n|n-1) = \sum_l w_l \mathcal{X}_l^{*}(n-1|n-1)\mathcal{X}_l^{*}(n-1|n-1)^{H}$$
$$-\hat{\mathbf{x}}(n|n-1)\hat{\mathbf{x}}(n|n-1)^{H} + \mathbf{GQG}^{H}$$

Update

- compute the Cholesky factor of $\mathbf{P}(n|n-1)$:

$$\mathbf{P}(n|n-1) = \mathbf{S}(n|n-1)\mathbf{S}(n|n-1)^{H}$$

- compute again the sigma points and the weights according to "Appendix 6" (Gauss-Hermite quadrature points for QKF) or according to "Appendix 7" (the cubature points for CKF).

- evaluate the sigma points:

$$\mathcal{X}_l(n|n-1) = \hat{\mathbf{x}}(n|n-1) + \mathbf{S}(n|n-1)\xi_l$$

- propagate the sigma points through the non-linear observation function:

$$\mathcal{Y}(n|n-1) = \mathbf{h}_n(\mathcal{X}_l(n|n-1)$$

- calculate $\hat{\mathbf{y}}^{-}(n|n-1)$:

Appendix 5: Quadrature Kalman filter and Cubature Kalman Filter

$\hat{\mathbf{y}}^{-}(n|n-1) = \sum_l w_l \mathcal{Y}(n|n-1)$

- update the Kalman gain:

$\mathbf{K}(n) = \{\mathbf{P}^{xy}\}\{\mathbf{P}^{yy}\}^{-1}$

where

$\mathbf{P}^{xy} = \sum_l w_l \mathcal{X}_l(n|n-1)\mathcal{Y}(n|n-1)^H - \hat{\mathbf{x}}(n|n-1)\hat{\mathbf{y}}^{-}(n|n-1)^H$

and

$\mathbf{P}^{yy} = \sum_l w_l \mathcal{Y}(n|n-1)\mathcal{Y}(n|n-1)^H - \hat{\mathbf{y}}^{-}(n|n-1)\hat{\mathbf{y}}^{-}(n|n-1)^H + \mathbf{R}$

- update the state vector:

$\hat{\mathbf{x}}(n|n) = \hat{\mathbf{x}}(n|n-1) + \mathbf{K}(n)\{\mathbf{y}(n) - \hat{\mathbf{y}}^{-}(n|n-1)\}$

- update the error covariance matrix:

$\mathbf{P}(n|n) = \mathbf{P}(n|n-1) - \mathbf{K}(n)\mathbf{P}^{\mathbf{yy}}(n)\mathbf{K}^H(n)$

Appendix 6: Calculation of Gauss-Hermite quadrature points and weights

- Set the number of hermite polynomial points m and thus U^m points where
U is the size of the state vector.

- generate a symmetric tridiagonal matrix with zero diagonal elements $\mathbf{J}$ such that:

$J_{i,i+1} = \sqrt{\frac{i}{2}}$ where $i = 1, \cdots, m$

- compute $\left\{\lambda_i\right\}_{i=1,\cdots,m}$, which are the eigenvalues of $\mathbf{J}$

- set $\xi_l = \sqrt{2}\lambda_i$.

- set $w_i = (e_i)_1^2$ where $(e_i)_1$ is the first element of the i^{th} normalized eigenvector of $\mathbf{J}$.

- extend the one-dimensional quadrature point set of m points in one dimension to
a lattice of U^m cubature points in U dimensions by using the product rule:

$\sum_{i_1,i_2,\cdots i_U} w_{i_1} w_{i_2} \cdots w_{i_U} f(x_1^{i_1}, x_2^{i_2}, \cdots x_U^{i_U})$

- the weights for these Gauss-Hermite cubature points are calculated
by the product of the corresponding one-dimensional weights.

- by changing the variable $\mathbf{x} = \sqrt{2}\boldsymbol{\Sigma} + \mu$ we get Gauss-Hermite weighted
sum approximation for multidimensional Gaussian integral where μ is the mean
and $\boldsymbol{\Sigma}$ is the covariance of Gaussian ($\boldsymbol{\Sigma} = \sqrt{\boldsymbol{\Sigma}}\sqrt{\boldsymbol{\Sigma}^{\boldsymbol{H}}}$).

- Then, let $\int c(\mathbf{x})\mathcal{N}\{\mathbf{x};\mu;\boldsymbol{\Sigma}\}d\mathbf{x} \approx \sum_{i_1,i_2,\cdots i_U} w_{i_1} w_{i_2} \cdots w_{i_U} f(\sqrt{\boldsymbol{\Sigma}}\xi_{i_1,i_2,\cdots i_U} + \mu)$.

- $w_{i_1,i_2,\cdots i_U} = \frac{1}{\pi^{m/2}} w_{i_1} w_{i_2} \cdots w_{i_U}$

- $\xi_{i_1,i_2,\cdots i_U} = \sqrt{2}(x_1^{i_1}, x_2^{i_2}, \cdots x_U^{i_U})$.

Appendix 7: Calculation of cubature points and weights

- Set the number of cubature points, $m = 2U$ where U is the size of the state vector.

-set $\xi_i = \sqrt{\frac{m}{2}}[\mathbf{1}]_i$ where $[\mathbf{1}]$ is i^{th} column of the matrix

$$[\mathbf{1}] = \begin{Bmatrix} 1 & 0 & \cdots & -1 & 0 & \cdots \\ 0 & 1 & \cdots & 0 & -1 & \cdots \\ \vdots & 0 & \cdots & \vdots & 0 & \cdots \\ 0 & 0 & \cdots & 0 & 0 & \cdots \end{Bmatrix}$$

- set the weight to $w_i = \frac{1}{m}$

References

1. FCC, (2002). Spectrum policy task force report, ET Docket, No 02-155.
2. Jovicic, A., & Viswanath, P. (2006). Cognitive radio: An information-theoretic perspective. In *Proceedings of the IEEE international symposium on information theory* (ISIT), pp. 2413–2417.
3. Chen, J., & Wen, C. (2010). A novel cognitive radio adaptation for wireless multicarrier systems. *IEEE Communications Letters*, *14*(7), 629–631.
4. Mitola, J. (2000). Cognitive radio: An integrated agent architecture for software defined radio. PhD thesis, Royal Institute of Technology (KTH) Sweden.
5. Goldsmith, A., Jafar, S., Maric, I., & Srinivasa, S. (2009). Breaking spectrum gridlock with cognitive radios: An information theoretic perspective. *Proceedings of the IEEE*, *97*(5), 894–914.
6. Agrawal, G., & Banerjee, A. (2013). Stable throughput of an interweave cognitive radio system employing SR-ARQ protocol. In *Proceedings of the European wireless conference* (EW), pp. 1–5.
7. Kouassi, B., Slock, D., Ghauri, I., & Deneire, L. (2013). Enabling the implementation of spatial interweave LTE cognitive radio. In *Proceedings of the EURASIP-European signal processing conference* (EUSIPCO), pp. 1–5.
8. Senthuran, S., Anpalagan, A., Hyung, Y., Karmokar, A., & Das, O. (2014). An opportunistic channel access scheme for interweave cognitive radio systems. *Journal of Communications and Networks*, *16*(1), 56–66.
9. Chakravarthy, V., Wu, Z., Temple, M., Garber, F., & Li, X. (2008). Cognitive radio centric overlay/ underlay waveform. In *Proceedings of the IEEE symposium on new frontiers in dynamic spectrum access networks* (DySPAN), pp. 1–10.
10. Mina, D., & Paeiz, A. (2012). Joint power and rate allocation in CDMA-based underlay cognitive radio networks for a mixture of streaming and elastic traffic. *EURASIP Journal on Wireless Communications and Networking*, *10*(262), 1–11.
11. Zhang, H., Ruyet, D., Roviras, D., & Sun, H. (2010). Capacity analysis of OFDM/FBMC based cognitive radio networks with estimated CSI. In *Proceedings of the international conference on cognitive radio oriented wireless networks communications* (CROWNCOM), pp. 1–5.
12. Jinhyung, O., & Wan, C. (2010). A hybrid cognitive radio system: a combination of underlay and overlay approaches. In *Proceedings of the IEEE vehicular technology conference* (VTC), pp. 1–5.
13. Abdou, A., Ferre, G., Grivel, E., & Najim, M. (2013). Interference cancelation in multiuser hybrid overlay cognitive radio. In *Proceedings of the EURASIP-European signal processing conference* (EUSIPCO).
14. Li, L., Khan, F., Pesavento, M., & Ratnarajah, T. (2011). Power allocation and beamforming in overlay cognitive radio systems. In *Proceedings of the IEEE vehicular technology conference* (VTC), pp. 1–5.
15. Ma, L., Liu, W., & Zeira, A. (2012). Making overlay cognitive radios practical. In *Proceedings of the IEEE international conference on acoustics, speech, and signal processing* (ICASSP), pp. 3145–3148.
16. Sun, S., Ju, Y., & Yamao, Y. (2013). Overlay cognitive radio OFDM system for 4G cellular networks. *IEEE Wireless Communications*, *20*(2), 68–73.
17. Dent, P., Bottomley, G., & Croft, T. (1993). Jakes fading model revisited. *Electronics Letters*, *29*(13), 1162–1163.
18. Young, D., & Beaulieu, N. (2000). The generation of correlated Rayleigh random variates by inverse Fourier transform. *Electronics Letters*, *48*(7), 1114–1127.
19. Grolleau, J., Grivel, E., & Najim, M. (2008). Two ways to simulate a Rayleigh fading channel based on a stochastic sinusoidal model. *IEEE Signal Processing Letters*, *15*, 107–110.
20. Jamoos, A., Grivel, E., Shakarneh, N., & Abdel Nour, H. (2011). Dual optimal filters for parameter estimation of a multivariate AR process from noisy observations. *IET Signal Processing*, *5*(5), 471–479.
21. Jamoos, A., Grivel, E., Christov, N., & Najim, M. (2009). Estimation of autoregressive fading channels based on two cross-coupled H infinity filters. *Signal, Image and Video Processing Journal*, *3*(3), 209–216.
22. Baddour, K., & Beaulieu, N. (2005). Autoregressive modeling for fading channel simulation. *IEEE Transactions on Wireless Communications*, *4*(4), 1650–1662.
23. Merchan, F., Turcu, F., Grivel, E., & Najim, M. (2010). Rayleigh fading channel simulator based on inner-outer factorization. *Signal Processing*, *90*(1), 24–33.
24. Simon, D. (2006). *Optimal state estimation Kalman, H1 and nonlinear approaches*. Hoboken: Wiley.
25. Wan, E., & Merwe, R. (2002). *Kalman filtering and neural networks - Chapter 7 the unscented Kalman filter*. Hoboken: Wiley.

26. Abdou, A., Turcu, F., Grivel, E., Diversi, R., & Ferré, G. (2015). Identification of an autoregressive process disturbed by a moving average noise based on inner- outer factorization, Signal, Image and Video processing (SIVP)-springer, Vol. 9, pp. 235–244.
27. Challa, S., Bar-Shalom, Y., & Krishnamurthy, V. (1999). Nonlinear filtering using Gauss-Hermite quadrature and generalised Edgeworth series. *Proceedings of the American Control Conference (ACC)*, *5*, 3397–3401.
28. Arasaratnam, I., & Haykin, S. (2009). Cubature Kalman filters. *IEEE Transactions on Automatic Control*, *54*(6), 1254–1269.
29. Fusco, T., Petrella, A., & Tanda, M. (2009). Data-aided symbol timing and CFO synchronization for filter bank multicarrier systems. *IEEE Transactions on Wireless Communications*, *8*(5), 2705–2715.
30. Poveda, H., Ferré, G. & Grivel, E. (2012). Frequency synchronization and channel equalization for an OFDM-IDMA uplink system. In *Proceedings of the IEEE international conference on acoustics, speech, and signal processing* (ICASSP), pp. 3209–3212.
31. Cadambe, V., & Jafar, S. (2008). Interference alignment and degrees of freedom of the K-user interference channel. *IEEE Transactions on Information Theory*, *54*(8), 3425–3441.

Publisher's Note Springer Nature remains neutral with regard to jurisdictional claims in published maps and institutional affiliations.

Ahmed Abdou received his B.Sc. degree in electronic engineering from Al-Quds University (Palestine) in 2004, M.Sc. degree in Electronic and communication engineering from Al-Quds University in 2008, and the Ph.D. degree in Signal processing and communication from Bordeaux 1 University (France) in 2014. His research interests are in the field of communication systems and signal processing for wireless communications and channel estimation techniques, and cognitive radio. He got many awards and scholarship during his study and in his current job as an assistant professor in signal processing and communication as well as the director of innovation department at Al-Quds University.

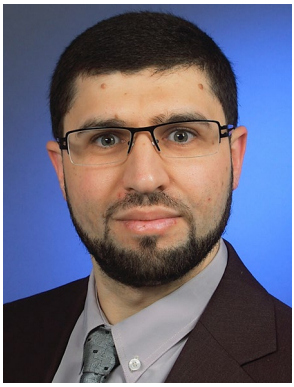

Ali Abdo received his B.Sc. degree in electronic engineering from Alquds University (Palestine) in 2005, M.Sc. degree in Power and Automation from University of Duisburg-Essen (Germany) in 2008, and the Ph.D. degree in electrical engineering at Institute for Automatic Control and Complex Systems (AKS), University of Duisburg-Essen in 2013. Mr. Abdo got many awards and scholarships throughout his study. His research interests include model-based fault diagnosis, fault tolerant control in electrical machines and fault detection in switched systems.

Ali Jamoos was born in Jerusalem, Palestine, in 1973. He received the BSc degree in electronic engineering from Al-Quds University, Jerusalem, in 1996; the MSc degree in communications from Jordan university of science and technology (JUST), Jordan, in 2000; the Ph.D. degree in signal processing and communications from Bordeaux 1 university, France, in 2007. His research interests are in the field of signal processing for wireless communications with focus on mobile fading channel modeling, estimation and equalization, multicarrier techniques, RFID systems, wireless sensor networks, cognitive radio, mobile network planning and optimization. He is an IEEE member since 2004. Currently, he is an associate professor at the department of the electronic and communication engineering at Al-Quds university.